Fluid Flow in Porous medium Based on Navier-Stokes Equation

Douglas Armstrong

Department of Mathematics and Computer Science Albion College, 611 E. Porter St., Albion, Michigan 49224, USA

E-mail: *DRA11@albion.edu*

Abstract

Rock porous medium is a medium to store and migrate oil, gas, coalbed methane, etc. The study of fluid flow laws in pore-scale porous medium has important theory significance and application value. The paper adopts the method of combining fluid dynamics and seepage mechanics. It creates a finite element calculation mesh of pore-scale porous medium on the basis of image processing technique, and simulates the distribution law of porous medium pressure and flow velocity in water drive process on COMSOL Multiphysics software platform, which is compared with the result of water displacing oil physical simulation experiment and verifies the feasibility of the method. Therefore, the research findings are of important theoretical significance in the development of reservoir fluid-solid coupling theory, oil-gas field and ground water.

1. Introduction

Seepage mechanics studies mainly focus on adopting macro research methods, i.e., taking rock or soil samples as well as formation or soil as the study object [1,2]. These studies, which are undoubtedly important and necessary, have reached a considerable degree not only in scale and but also in depth. However, it is still hard to solve many other problems, especially those about seepage mechanism methods if only by means of macroscopic research. The microscopic study of seepage mechanism and its complementation with macro research will contribute to the satisfactory resolution of some relevant issues.

Microscopic physical simulation experiment was started from two-dimensional study and mainly observed the details, mechanics and laws within transparent two-dimensional models with the help of microscopic video technology. Meanwhile, it measured the micro-flow synchronously through the use of two-phase and three-phase micro determinator. Started earlier in China, the thought of "microscopic measure" was proposed by CAS's Institute of Porous Flow and Fluid Mechanics in 1967. In 1979, it began the study and development of two-dimensional physical simulation technology to test technology and equipment as well as two-dimensional micro-seepage experiment. They took the lead in publishing their research findings on microscopic seepage nationally and internationally in 1984 and published micro-flow monograph in 1990. They applied the simulation test technology to the study of multiphase seepage, non-Newtonian fluid seepage, physical and chemical seepage and non-isothermal flow system, by which some new seepage mechanisms and laws were found. Thus they could specify, improve and systematize those unspecific and less systematic mechanisms and laws. There has been a number of

achievements in recent years on microphysical simulation of three-dimensional porous media flow at home and abroad with the help of computer micro-tomography technology [3-8].

However, microscopic physical simulation experiment has its own disadvantages such as higher cost, more time consuming, fewer considerable factors and so on. By studying pore-scale percolation mechanism, seepage field is controlled by many factors including pores' boundary conditions, viscous force, capillary force, gravity and complex physicochemical processes. Under such complicated background[9-12], the better approach to solve the problem is to idealize the rock porous medium as some kind of abstract lattice or mesh. This idea made people put forward several kinds of methods in the microscopic numerical simulation of porous medium in which there are mainly Lattice Boltzmann method and pore scale network model. Originated from simulated calculation of Brownian motion, Lattice Boltzmann method has a tinier simulation scale and more complex numerical calculation. The U.S. national laboratory Los Alamos applied Lattice Boltzmann method to simulate two-dimensional flow in rock pores and figured out the relative permeability curves and residual oil saturation. CAS's Institute of Poromechanics and Mechanics applied this method [13-14] to the study of slippage effect of gas seepage and relative permeability curves of oil-water two-phase seepage showing that the results were in good agreement with the experimental values. Pore scale network model, which has a wider simulation scale and is more practical in application, stemmed from the study of gas seepage of porous carbon medium in gas mask. Fatt was the first one to study the dynamic and static two-dimensional grid of porous medium in the pore scale network model. Later other scholars improved and developed the model. For instance, the University of Southern California combined network model with scanning electron microscopy techniques and found the method to get pore parameters.

Petro China Research Institute of Petroleum Exploration and Development figured out oil-water relative permeability curves on the use of irregular network model. Besides, they studied the effects of pore radius, pore distribution and coordination number by percolation theory. Both Lattice Boltzmann method and pore scale network model (i.e.percolation method) which have achieved certain development used computers to simulate pore scale seepage.

The paper built a mathematical model of fluid flow in porous medium on the basis of hydrodynamics theory [15-17] and finite calculation grid on the basis of image processing technology. The basic fluid flow laws of porous medium was acquired by numerical simulation and compared with the result of water-drive physical simulation experimental result, which finally verified its feasibility.

2. Mathematical model of pore scale flow

Suppose it is compressible fluid in rock pores and laminar fluid flow, establish a pore scale flow mathematical model based on hydromechanical N-S equations without regard to deformation of porous medium.

2.1 One-phase incompressible liquid flow mathematical model in elastic porous medium

According to law of conservation of mass, continuous equation of fluid flow in porous medium can be expressed as:

$$\rho \frac{\partial \phi}{\partial t} + \phi \frac{\partial \rho}{\partial t} + \frac{\partial (\rho v_x)}{\partial x} + \frac{\partial (\rho v_y)}{\partial y} = 0 \qquad (1)$$

As seepage process changes continuously and reservoir rock matirx is flexible, the mechanical property of fluids within pores and the solid rock matrix will change along with the changing state. At the moment, a state equation is a need to describe the change of mechanical properties aroused by the flexibility.

If the fluid in pores is elastic, then:

$$\rho = \rho_0[1 + C_\rho(p - p_0)] \tag{2}$$

In the formula: Cp= elastic compressibility of density.

Plug (2) into (1):

$$\rho_0 \phi C_\rho \frac{\partial p}{\partial t} + \frac{\partial(\rho v_x)}{\partial x} + \frac{\partial(\rho v_y)}{\partial y} = 0 \tag{3}$$

Formula (3) is the one-phase compressible liquid flow's mathematical model in porous medium.

2.2 Motion equation

Two-dimensional viscous compressible liquid flow's differential equation of motion (N-S equation) is as shown in formula (4):

$$\left.\begin{aligned}
\rho\frac{\partial v_x}{\partial t} &= \rho f_x - \frac{\partial p}{\partial x} + \frac{\partial}{\partial x}(\mu\frac{\partial v_x}{\partial x}) + \frac{\partial}{\partial y}(\mu\frac{\partial v_x}{\partial y}) + \frac{\partial}{\partial x}[\frac{\mu}{3}(\frac{\partial v_x}{\partial x} + \frac{\partial v_y}{\partial y})] \\
\rho\frac{\partial v_y}{\partial t} &= \rho f_y - \frac{\partial p}{\partial y} + \frac{\partial}{\partial x}(\mu\frac{\partial v_y}{\partial x}) + \frac{\partial}{\partial y}(\mu\frac{\partial v_y}{\partial y}) + \frac{\partial}{\partial y}[\frac{\mu}{3}(\frac{\partial v_x}{\partial x} + \frac{\partial v_y}{\partial y})]
\end{aligned}\right\} \tag{4}$$

In the formula: μ = dynamic viscosity of fluid.

Two-dimensional viscous incompressible liquid flow's differential equation of motion (N-S equation) is as follows:

$$\left.\begin{aligned}
\frac{\partial v_x}{\partial t} + v_x\frac{\partial v_x}{\partial x} + v_y\frac{\partial v_x}{\partial y} &= f_x - \frac{1}{\rho}\frac{\partial p}{\partial x} + \frac{\mu}{\rho}(\frac{\partial^2 v_x}{\partial x^2} + \frac{\partial^2 v_x}{\partial y^2}) \\
\frac{\partial v_y}{\partial t} + v_x\frac{\partial v_y}{\partial x} + v_y\frac{\partial v_y}{\partial y} &= f_y - \frac{1}{\rho}\frac{\partial p}{\partial y} + \frac{\mu}{\rho}(\frac{\partial^2 v_y}{\partial x^2} + \frac{\partial^2 v_y}{\partial y^2})
\end{aligned}\right\} \tag{5}$$

In the formula: $\dfrac{\mu}{\rho}$ = kinematic viscosity of fluid, which can be directly replaced by υ.

2.3 Boundary conditions

Boundary condition are classified as constant pressure boundary and fixed flow boundary. The constant pressure boundary is defined as the pressure of each point on the boundary is known at every moment or the bottom hole pressure of the well is known. If it is the given function $f_1(x, y)$, then:

$$p_g = f_1(x, y, t) \tag{6}$$

In the formula: p_g = the pressure of (x, y) at the moment of t.

Fixed flow boundary is defined as the flow on the boundary is known. If it is the known function $f_2(x, y)$ on the given boundary, then:

$$\left.\frac{\partial p}{\partial \vec{n}}\right|_{g} = f_2(x, y, t)$$

(7)

In the formula: $\vec{n}$ = directional derivative of outer normal direction of the pressure on the boundary.

When $t = 0$, the initial pressure and saturation distribution in oil layer can be showed as:

$$p(x, y, 0) = p_0(x, y)$$

(8)

$$s(x, y, 0) = s_0(x, y)$$

(9)

## 3. Rock pore structural modeling based on digital image

This paper processed the images processing with the use of the toolbox of MATLAB [18,19]. Figure1 (a) is the SEM image of a rock, in which green areas represent the solid rock matrix and black areas represent the pore structure. Firstly, turn Figure1 (a) into grey-scale and get Figure1 (b) by equalization and binarization processing. Secondly, filter Figure1 (b) and get Figure1 (c). Finally, process Figure1 (c) by erosion or dilation and get a new Figure1(d).
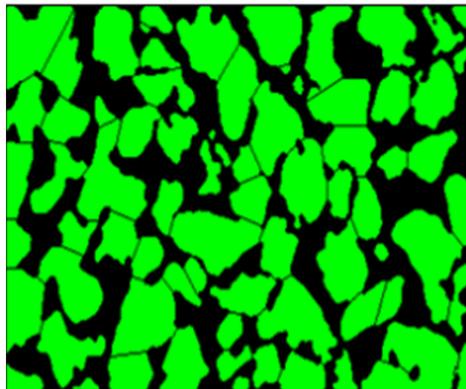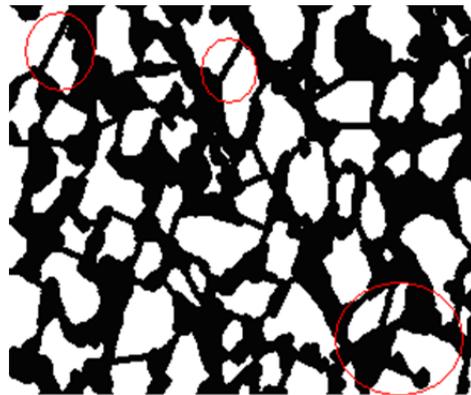

(a) Original SEM image
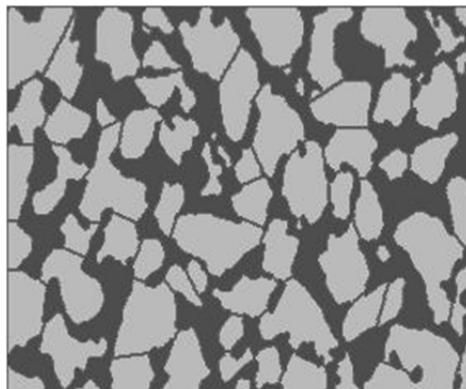

(b) Processed grey-scale image
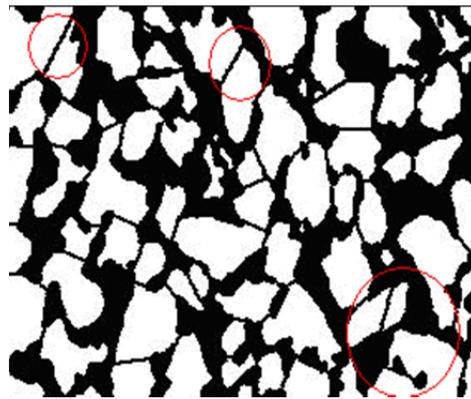
(c) Filtered image

(d) Dilation processed image

Fig. 1 MATLAB Image Processing

The images above are all bitmaps, which are needed to change into vectograms to generate finite element mesh. After obtaining the vectograms with the help of Algolab Raster to Vector Conversion Toolkit, a good finite element mesh model can be built with the use of COMSOL Multiphysics. Figure2 shows the finite element mesh model.
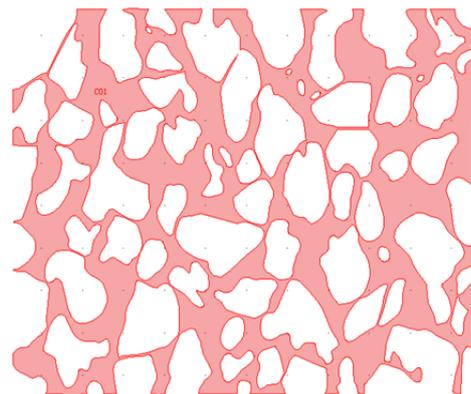

(a) Pore scale model
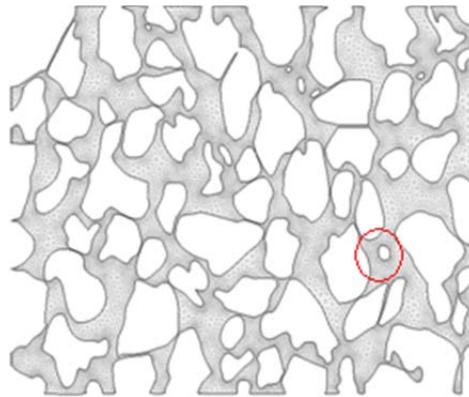
(b) Finite element mesh model

**Fig.2** Diagram of Generation process of finite element mesh model

4. Numerical simulation of pore scale flow field

4.1 Numerical model

Do an experimental analysis of the core at 1000 meters below the reservoir rock and get core No.1's SEM images [20]. Choose one of them as shown in Figure3. Use the digital image processing method mentioned above to obtain the numerical model of rock pore with a mesh number of 23430 as shown in Figure4. Use N-S equation as the governing equation of the fluid motion in pores and build a numerical model of flow field of two dimensional pore scale.
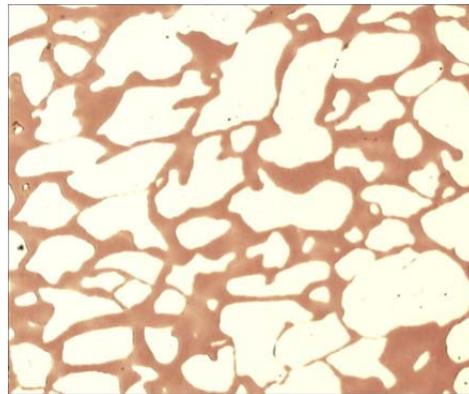
Fig. 3 SEM image of rock
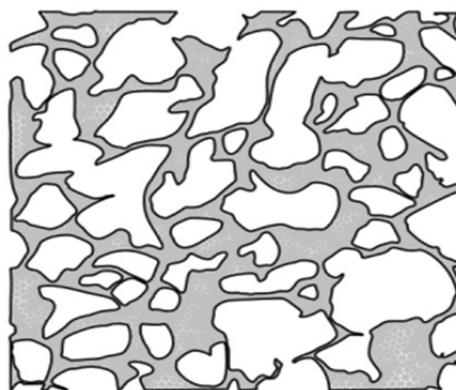
Fig. 4 Numerical model of rock pore

4.2 Calculating parameter and boundary conditions

The main direction of the fluid flow in pores is from left to right or from right to left, which is a laminar flow type. It is the known flowing pressure of inlet and outlet without regard to volume force caused by gravity. Suppose it is a symmetric flow for the upper and lower boundary, and there is a certain fluid density and constant temperature, the fluid in pores can be described by the incompressible N-S equation. The boundary setting is as shown in Table 1.

Table 1 Boundary setting

Boundary type	Boundary setting	Value	Mathematical model
outlet	pressure, viscous stress	$p=p_2$	$\vec{n} \cdot \eta \left(\nabla \vec{u} + \left(\nabla \vec{u} \right)^T \right) = 0$
inlet	pressure, viscous stress	$p=p_1$	$\vec{n} \cdot \eta \left(\nabla \vec{u} + \left(\nabla \vec{u} \right)^T \right) = 0$
grain walls	wall, no slip	-	$\vec{u} = 0$
symmetric boundary	symmetry	-	$\vec{n} \cdot \vec{u} = 0$ $\vec{t} \cdot \left[-pI + \eta \left(\nabla \vec{u} + \left(\nabla \vec{u} \right)^T \right) \right] \vec{n} = 0$
rigid wall	no slip	-	-

In the calculations above, pressures on the boundary of inlet and outlet are known. The pressure on the boundary of inlet is $p1=7.15Pa$, $p2=0Pa$. $\eta =0.001$ kg/(m·s), $\rho =1000$ kg/m³, $\lambda =0.33$, E=6.0×109Pa, with a corresponding macro pressure gradient of 0.013MPa/m.

5. Results and analysis

Figure5 is a calculated nephogram of pressure distribution where the inlet is on the right boundary and outlet on the left boundary. The blue part stands for low pressure area while red part stands for high pressure area. The analysis of it can draw the following conclusions [21-23]:

(1) The pressure decreases constantly in the process of fluid flow.

(2) The pressure varies unobviously in the area of big pores and thick pore throats, while its distribution varies obviously in the region where the throat radius changes visibly.
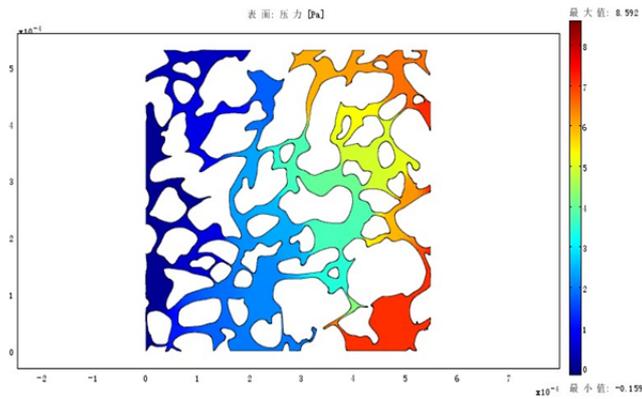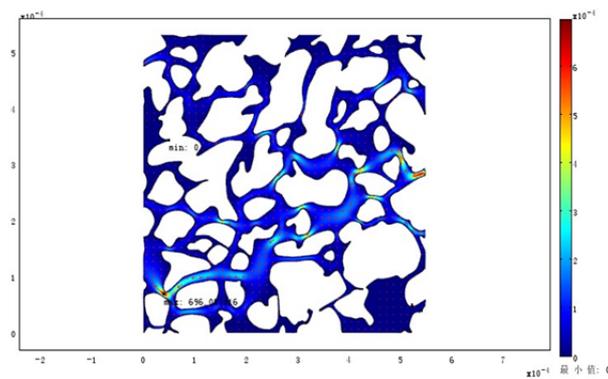
Fig. 5 Nephogram of pressure distribution

Fig. 6 Velocity distribution nephogram of pore fluid

Figure 6 shows the velocity field of fluid within pores. Different colors stand for a different velocity magnitudes, in which the red arrows indicate the moving direction of the fluid. Conclusions are summarized as follows:

(1) As expected, the highest flow velocity occurs in the narrowest pores of the inlet. It decreases at a slower pace in areas where there occurs a crossed extension and increasing flow. And it doesn't change obviously in narrow channels.

(2) The highest velocity nearly occurs in the same point for the two simulation results, with an approximate velocity difference of 1.7720%. The position where it appears has nothing to do with the symmetric boundary of inlet and outlet. It is the pore-throat ratio that is the determining factor of velocity.

Figure7 is a streamline chart of the flow field. The red lines show the fluid's motion trajectory within pores. Conclusions are summarized as follows:

(1) No matter whether the outlet is on the right or on the left boundary, the fluid's motion trajectory is almost the same;

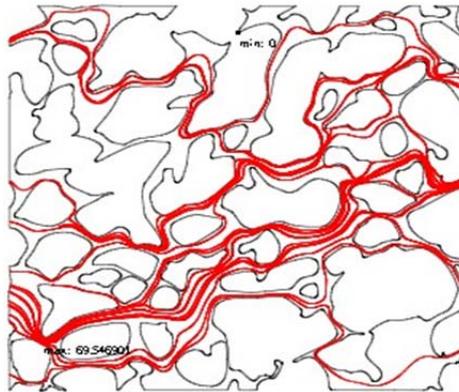(2) The fluid in pores always flows along the long and narrow throat that connects big pores.

Fig. 7 Streamline chart of flow field
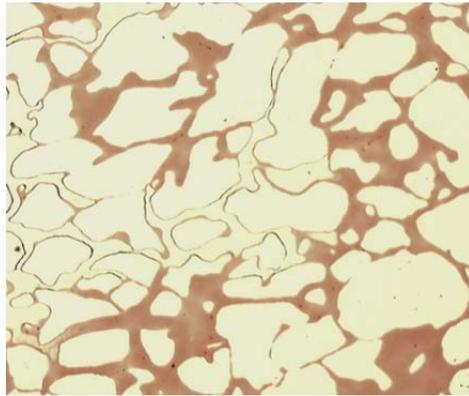
6. Results comparison

Use the rock core slice model to do a water drive physical simulation experiment to verify the correctness of the numerical simulations above, just as Figure8 showing the dynamic changes of water displacement. In Figure8, white area represents solid rock matrix, brown area stands for rock pores. After injecting waters, brown areas are gradually replaced by milk yellow areas indicating the fluid flow into the pore's throat path. (a)~(g) in Figure8 shows the fluid flow's process at different time points, in which the inlet is on the left boundary. The final result is displaced in (g) where residual brown areas, i.e. the blind ends, show they are not flowed through by the fluids. (h) is the numerical simulation result-a streamline chart of the velocity field.
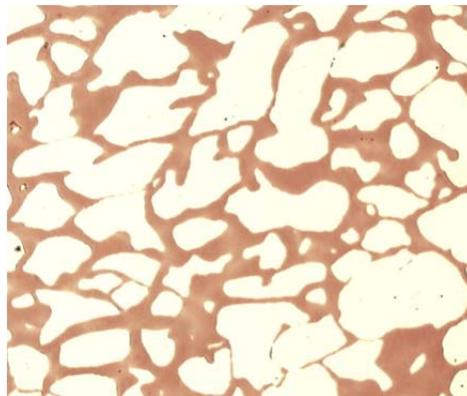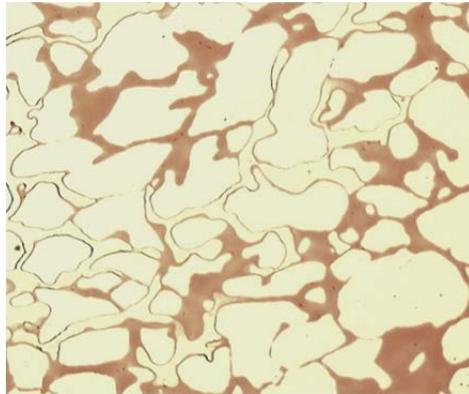

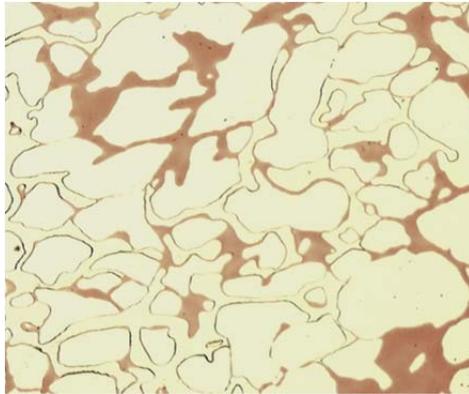
(a) Before water injection
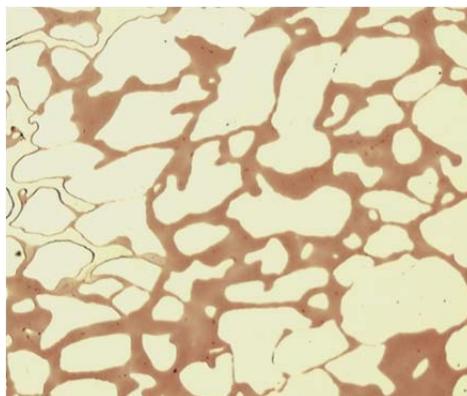
(b) At the time node of 1p.m.
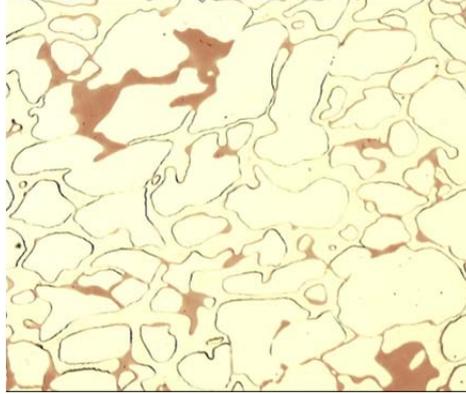
(c)　At the time node of 2p.m.
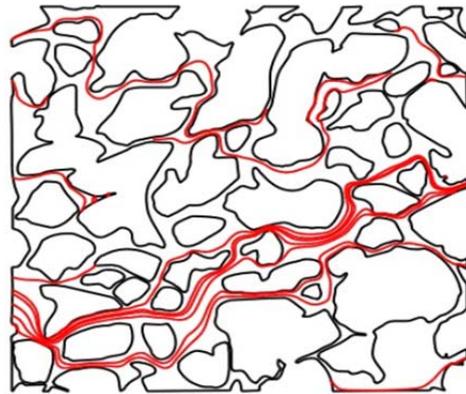

(d)　At the time node of 3p.m.

(e)　At the time node of 4p.m.

(f) At the time node of 5p.m.

(g) At the time node of 6p.m.

(h) Numerical simulation result

Fig. 8 Results comparing

The flow path when injecting water can be found in displacement images at the different time nodes. When the time node is at 2p.m., there is only a small amount of fluid flowing into the pore throat path at the lower left corner of the area while pores in the middle area are almost filled with water. When it is at the time node of 4p.m., the lower left corner is full of water, and the streamline has arrived at the middle area at the same time. It indicates that fluid velocity in the lower area of flow field is much more faster than that in the upper, which matches the numerical simulation as well.

Comparing the result of water drive physical simulation with the experiment result, we can find that the flow trend after water injection is the same as that of numerical simulation. Therefore, it can be concluded that the numerical simulation results of pore scale flow field are consistent with the experiment results of the core No.1. Meanwhile it also proved the feasibility of the method of by pore structure modeling based on digital image.

Conclusions

(1) Based on fluid dynamics theory, compressible liquid flow mathematical model in elastic porous medium was built;

(2) Using digital image processing technology, a method of establishing two-dimension pore scale numerical model of flow and deformation was given;

(3) Through numerical simulation of fluid flow in pore scale, some results have been obtained, such as the distribution nephogram of pressure and the velocity field, streamline chart, which have been compared with the results of displacement of oil by water experiment. It proved that it was very effective.

References

[1] Zhe-tan Luo, Yun-cheng Wang. Pore Structure in Oil and Gas Reservoir. Beijing: Science Press (1986)

[2] Brian Berkowitz, Robert P. Ewing. Percolation Theory and Network Modeling Applications in Soil Physics. Surveys in Geophysics, 19,23-72 (1998)

[3] Ping-ping Shen. Flow and Transport of Oil and Water in Porous Media. Beijing: Petroleum Industry Publishing House (2000)

[4] Jun Yao, Xiu-cai Zhao, Yan-jing Yi, Jun Tao. Analysis methods for reservoir rock's microstructure. *Journal of China University of Petroleum*, 31(1), 80-86 (2007)

[5] S. Roels, J. Elsen, J. Carmeliet and H. Hens. Characterization of Pore Structure by Combining Mercury Porosimetry and micrography. *Materials and Structures Materials at Constructions*, 34(3), 76-82 (2001)

[6] Carl Sisk, Elizabeth Diaz,Joel Walls, Avrami Grader and Michael Suhrer. 3D Visualization and Classification of Pore Structure and Pore Filling in Gas Shales. SPE134582, SPE Annual Technical Conference and Exhibition (2010)

[7] Shang-ping Guo, Yan-zhang Huang, Juan Zhou, Pei-qiong Kuang. Microscopic Research of the Flow of Physical Fluid through Porous Media. *Chinese Journal of Theoretical and Applied Mechanics*, 18(S1), 45-50 (1986)

[8] Jian-jun Liu, Xian-gui Liu, Xia-ting Feng. Physical simulation of Water-oil Microcosmic Flow through Fracture Porous Media. *Chinese Journal of Rock Mechanics and Engineering*, 22(10), 1646-1650 (2003)

[9] Yang Baohua, Wu Aixiang, Jiang Huaichun. Evolvement of permeability of ore granular media during heap leaching based on image analysis. *Transaction of Nonferrous Metals Society of China*, 18(2), 426-431 (2008)

[10] P. Baud, S. Vinciguerra, C. David, A. Cavallo, E. Walker and T. Reuschle. Compaction and Failure in High Porosity Carbonates: Mechanical Data and Microstructural Observations. Pure appl. *Geophys*, (166), 869-898 (2009)

[11] Rosolino Cirrincione, Eugenio Fazio, Patrizia Fiannacca, Gaetano Ortolano and Rosalda Punturo. Microstructural Investigation of Naturally Deformed Leucogneiss from an Alpine Shear Zone (Southern Calabria-Italy). *Pure and Applied Geophysics*, (166), 995-1010 (2009)

[12] Mark A. Knackstedt, Adrian P. Sheppard, Muhammad Sahimi. Pore network modelling of two-phase flow in porous rock: the effect of correlated heterogeneity. *Advances in Water Resources*, (24), 257-277 (2001)

[13] Blunt M. J, Jaekson M.D., Piri M. Detailed Physics, Predictive capabilities and Macroscopic Consequences for Pore-network Models of Multi-Phase Flow. *Advances in Water Resources*, 25(8-12), 1069-1089 (2002)

[14] Jun Yao, Jun Tao, Ai-fen Li. Research on oil-water two-phase flow using 3D random network model. *ACTA PETROLEI SINICA*, 28(2), 94-97 (2007)

[15] Xie Jianbin, Fan Jing, Liu Wenlian. Dynamic Stability of the Tailings Dam under High Intensity Seismic Load Coupled with the Effect of Seepage. *Disaster Advances*,5(4), 1611-1616 (2012)

[16] Yin Guangzhi, Jiang Changbao, Xu Jiang. Experimental study of Solid-liquid-gas coupling seepage of containing-gas coal. *Disaster Advances*, 4(S1), 103-108 (2011)

[17] Jiang Changbao, Yin Guangzhi, Xu Jiang. Experimental Study of the Influence on Mechanical Properties and Coalbed Methane Seepage of Coal Reservoir Face Cleat. *Disaster Advances*, 3(4), 487-494 (2010)

[18] Liu Jianjun, Sano Yoshihiko, Nakayama Akira. A simple mathematical model for determining the equivalent permeability of fractured porous media. *International Communications in Heat and Mass Transfer*, 36, 220-224 (2009)

[19] Liu Jianjun, Lin Lijun, Pei Guihong. Using Rock SEM Image to Create Pore-scale Finite Element Calculation Mesh. *Physics Procedia*, 22, 227-232 (2011)

[20] Liu Jianjun, Li Quanshu. Numerical simulation of injection water flow through mudstone interlayer in low permeability oil reservoir development. *Disaster Advances*, 5(4),962-967 (2012)

[21] S.R.Tod. The effects of stress and fluid pressure on the anisotropy of interconnected cracks. *Geophys.J Int*.,(149), 149-156 (2002)

[22] Ki-Bok Min, J Rutqvist, Chin-Fu Tsang and Lanru Jing. Stress-Dependent Permeability of Fractured Rock Masses: A Numerical Study. *International Journal of Rock Mechanics & Mining Sciences*, 41(7), 1191-1210 (2004)

[23] Liu Xiaoli, Wang Enzhi, Han Guofeng. Discontinuous Deformation Analysis for the Slope Stability in Jinping First Stage Hydropower Station, Southwestern China. Disaster Advances, 5(4), 1394-1399 (2012)